JOURNAL OF NEUROTRAUMA 31:1776–1788 (November 1, 2014)

DOI: 10.1089/neu.2014.3388

Bilateral Contusion-Compression Model of Incomplete Traumatic Cervical Spinal Cord Injury

Nicole Forgione,[1] Spyridon K. Karadimas,[1,2] Warren D. Foltz,[3,4] Kajana Satkunendrarajah,[1] Alyssa Lip,[2] and Michael G. Fehlings[1,2,5,6]

Abstract

Despite the increasing incidence and prevalence of cervical spinal cord injury (cSCI), we lack clinically relevant animal models that can be used to study the pathomechanisms of this injury and test new therapies. Here, we characterize a moderate cervical contusion-compression model in rats that is similar to incomplete traumatic cSCI in humans. We characterized the effects of 18-g clip-compression injury at cervical level C6 over an 8-week recovery period. Using Luxol fast blue/hematoxylin-eosin staining in combination with quantitative stereology, we determined that 18-g injury results in loss of gray matter (GM), white matter (WM), as well as in cavity formation. Magnetization transfer and T2-weighted magnetic resonance imaging were used to analyze lesion dynamics *in vivo*. This analysis demonstrated that both techniques are able to differentiate between the injury epicenter, subpial rim, and WM distal to the injury. Neurobehavioral assessment of locomotor function using Basso, Beattie, and Bresnahan (BBB) scoring and CatWalk revealed limited recovery from clip-compression injury at C6. Testing of forelimb function using grip strength demonstrated significant forelimb dysfunction, similar to the loss of upper-limb motor function observed in human cSCI. Sensory-evoked potentials recorded from the forelimb and Hoffman reflex recorded from the hindlimb confirmed the fore- and hindlimb deficits observed in our neurobehavioral analysis. Here, we have characterized a clip-compression model of incomplete cSCI that closely models this condition in humans. This work directly addresses the current lack of clinically relevant models of cSCI and will thus contribute to improved success in the translation of putative therapies into the clinic.

Key words: cervical spinal cord injury; forelimb function

Introduction

Cervical spinal cord injury (cSCI) accounts for approximately 55% of all traumatic spinal cord injury (SCI).[1] In addition to the level of injury, the severity of injury is a key factor in determining the potential for recovery and course of treatment. Approximately 60% of traumatic SCI is classified as incomplete.[2] Though there have been vast improvements in the medical and surgical management of traumatic SCI, we currently lack therapies that can generate meaningful functional recovery, beyond what occurs naturally. The greatest hurdles to improved treatment are a critical knowledge gap with respect to the pathophysiology of incomplete SCI in the cervical region, as well as the lack of clinically relevant models that can be used to investigate potential therapies. A number of rodent cervical injury models, each with individual benefits and drawbacks, have previously been described. Some commonly used cervical injury models include sharp transection and blunt injury. Sharp transection results in complete severing of axons and is ideal for studying regeneration. This approach has yielded important insights into the mechanisms responsible for forelimb recovery after cervical injury in the rat.[3] However, these models do not allow for the study of mechanisms involved in incomplete SCI and reflect only a small proportion of human SCIs that occur as a result of sharp, penetrating injuries.[4]

Unilateral blunt trauma has proven successful in creating focal injuries using biomechanical forces similar to those that contribute to human SCI.[5,6] The primary drawback of this approach is that it typically relies on the use of a mechanical impactor, which does not recreate the sustained compression observed in human SCI. The use of a modified aneurysm clip has proven the most effective at

[1]Division of Genetics and Development, Toronto Western Research Institute, Krembil Neuroscience Center, University Health Network, Toronto, Ontario, Canada.
[2]Institute of Medical Sciences, Faculty of Medicine, University of Toronto, Ontario, Canada.
[3]Radiation Medicine Program, Princess Margaret Hospital, Toronto, Ontario, Canada.
[4]STTARR Innovation Center, University Health Network, Toronto, Ontario, Canada.
[5]Neuroscience Program, University of Toronto, Toronto, Ontario, Canada.
[6]Department of Surgery, Division of Neurosurgery, University of Toronto, Toronto, Ontario, Canada.

consistently generating injuries that model the acute impact and continuing compression observed in clinical SCI.[7] To study the effects of injury in the cervical cord, we have chosen a clip-compression model so as to recreate the hemorrhage, necrosis, ischemia, and inflammation triggered by physical trauma to the spinal cord that occurs in humans. Further, clip-compression injury models the partial axon severing and preservation of white matter (WM) tracts that are key features of incomplete SCI. We employed a moderate (18-g) injury at the C6 level to study neurobehavioral and neuroanatomical recovery for 8 weeks postinjury. Neuroanatomical recovery was assessed using quantitative lesion analysis and magnetic resonance imaging (MRI). Here, we demonstrate that T2-weighted imaging and magnetization transfer (MT)-MRI are useful tools for studying the neuroanatomy of the injured cord *in vivo*.

One of our primary aims was to create a model that has neurobehavioral similarities to humans with incomplete cSCI. The American Spinal Injury Association Impairment Scale provides the main criteria for the classification of injury severity.[8] Complete SCI is defined by the absence of motor and sensory function in the lowest sacral levels (S4–S5). In contrast, incomplete SCI is characterized by sparing of motor and/or sensory function at S4–S5. Many clinical studies have shown that patients with incomplete injuries experience natural recovery of sensory and motor function.[9] Recovery of upper-limb function has a significant effect on quality of life for patients with cSCI and, accordingly, has been identified as a priority by patients with tetraplegia.[10] Clinical studies have detailed unique recovery profiles in the upper limbs that are likely a result of the involvement of distinct mechanisms for upper-limb recovery.[11] Using Basso, Beattie, and Bresnahan (BBB) scoring to provide a general picture of locomotor deficits,[12] automated gait analysis with CatWalk,[13] grip strength testing to assess neuromuscular function in the forelimbs,[14,15] analysis of sensory-evoked potentials (SEPs), and Hoffman (H) reflex, we demonstrate the following neurobehavioral characteristics that are similar to functional deficits observed in humans with incomplete cSCI: 1) decreased hind- and forelimb motor function, accompanied by some sparing; 2) impairment of forelimb sensory function, with some sparing; 3) distinct recovery profiles of the fore- and hindlimbs; and 4) below-level spasticity.

Thus, our model provides a clinically relevant paradigm that will allow for greater insight into the pathophysiology of incomplete cervical injury and the identification of therapies targeted at improving functional recovery after cSCI.

Methods

Animal care

Adult female Wistar rats (250–300 g) for this study were obtained from Charles River Laboratories (Wilmington, MA). All animal care procedures were designed in accord with the *Guide to the Care and Use of Experimental Animals* established by the Canadian Council of Animal Care and were approved by the University Health Network Animal Care Committee.

Clip-compression spinal cord injury

This study made use of the aneurysm clip-compression model of SCI that has been extensively characterized in our laboratory. Animals were anesthetized using inhalant isoflurane (1–2%) delivered in a 1:1 mixture of O_2/N_2O. The surgical area was prepared by shaving and disinfection using isopropanol. A mid-line skin incision was made in the cervical area (C5–T2), and the three muscle layers overlaying the vertebrae were individually retracted. Animals received a C6–C7 laminectomy in preparation for 18-g clip-compression injury (Walsh, Oakville, Ontario, Canada) at the C6 spinal level lasting 1 min. A small square of Surgifoam® (Ethicon Endo-Surgery, Inc., Cincinnati, OH) was placed over the injury site, and the overlaying muscle and skin was sutured. Postoperatively, animals were treated with analgesics, anti-inflammatories, and saline (0.9%; 5 mL) to prevent dehydration. Animals were housed individually in standard rat cages with absorbent bedding at a temperature of 27°C for recovery. Injured animals had their bladders manually expressed three times daily until natural bladder function returned.

Neurobehavioral testing

Basso, Beattie, and Bresnahan open-field locomotion score. The general locomotor ability of animals was assessed using the BBB Locomotor Rating Scale. For this measure, rats are placed individually in an open field where locomotion can be assessed by two observers. Hindlimb locomotor function is scored using a 22-point (0–21) scale that evaluates parameters including joint movement, stepping ability, coordination, and trunk stability. Animals displaying normal locomotion receive a score of 21. Animals were scored once per week by two independent observers.

Inclined plane test

Animals are placed individually on a 28×30 cm board covered with a grooved rubber surface, and their ability to maintain body position is observed as the board is incrementally raised to increasing angles. The angle of incline is continually increased toward a vertical position until the animal can no longer maintain stability. A score is assigned by recording the greatest angle of incline at which the animal can maintain a stable body position for 5 sec. Animals were scored once per week.

Hand grip strength test

This test is used to assess forelimb motor function based on the ability of the animal to exert a pulling force on a metal grid attached to an electronic grip strength meter (SDI Grip Strength System, model DFM-10; San Diego Instruments, San Diego, CA). Animals were tested once per week, and each trial consisted of five separate pulls. The highest and lowest forces were omitted and the remaining three were averaged.

Automated gait analysis (CatWalk)

Gait analysis was carried out using the CatWalk system (Noldus Information Technology, Wageningen, The Netherlands).[13] Briefly, as animals traverse a horizontal glass plate, their footfalls are recorded by a video camera positioned beneath the walkway. Data files were collected and analyzed using version 7.1 of the CatWalk software. For analysis, crossing speed was standardized, and one uninterrupted crossing of the walkway was required. Individual paw prints were labeled by one observer blinded to the groups. Recordings were taken at 2, 4, 6, and 8 weeks postinjury. We selected the following parameters for analysis: stride length, print area, print width, print length, swing speed, maximum area of contact, and intensity. For all parameters, data analysis was performed with a threshold value of 25. Paw intensity was measured in arbitrary units (with a possible range of 0–250).

Tissue processing

After an overdose of isoflurane, animals were transcardially perfused using 4% paraformaldehyde (PFA) in phosphate-buffered saline (pH 7.4). Spinal cords were removed, placed in 4% PFA overnight at 4°C and transferred to 30% sucrose the next day. A

2 cm portion of the cervical spinal cord centred on the injury was embedded on dry ice using tissue-embedding medium (Shandon M-1; Thermo Scientific, Waltham, MA). Tissue sections were cut at a thickness of 30 μM using a cryostat and mounted on charged glass slides.

Quantitative lesion analysis

The cervical enlargement was serially sectioned, in a transverse plane, at intervals of 30 μM. The cellular stain hematoxylin-eosin (H&E) was used in combination with the myelin-specific stain, Luxol fast blue (LFB), to distinguish between gray matter (GM), white matter (WM), lesional tissue, and cavity. A total of 3.6 mm of cord was sampled every 360 μM. Volume measurements were obtained for individual tissue sections using the Cavalieri method of Stereo Investigator software (MBF Bioscience, Williston, VT). The percentage of preserved WM and GM, lesional tissue, and cavity was determined by dividing the volume of GM, WM, and lesional or cavity by the total volume of the cord.

Three-dimensional reconstruction of the spinal cord

Three-dimensional (3D) reconstructions were completed using Neurolucida software (MBF Bioscience, Williston, VT). Reconstructions were generated based on contours for the total cord (green), GM (yellow), lesional tissue (pink), and cavity (blue). Contours were traced using LFB-H&E-stained spinal cord sections. Reconstructions were based on data from three histological sections (30 μM thick) separated by an interval of 360 μM and thus represent a 1-mm section of the cord.

In vivo *electrophysiology*

Forelimb sensory-evoked potentials. Forelimb SEPs were recorded from naïve rats and C6-injured rats at 8 weeks post-injury. Recordings were carried out under isoflurane anesthesia with the animals positioned in a stereotactic holder in a prone position. The ligamentum flavum was removed between C1 and C2 to allow for two pairs of 1.0-mm ball electrodes to be placed extradurally over the spinal cord. The forepaw was stimulated by two stainless-steel needle electrodes using a constant current 0.1 ms in duration and 2.0 mA in intensity applied at a rate of 5.7 Hz. A total of 2000 SEPs were averaged and replicated at a bandwidth of 10–3000 Hz. SEP peak latency was measured from the initiation of stimulus (S) to the peak of the first negative peak (N1). Amplitudes were calculated as the voltage difference from the peak of the first positive peak (P1) to the peak of the first negative peak (N1).

Hoffman reflex recording. As with SEPs, H-reflex data were obtained from naïve rats and C6-injured rats 8 weeks postinjury. Under isoflurane anesthesia, recording electrodes were positioned 2 cm apart in the mid-calf region and the posterior tibial nerve was stimulated in the popliteal fossa using a 0.1-ms duration square wave pulse at a frequency of 1 Hz. The recordings were filtered between 10 and 10,000 Hz. H-reflex is a representation of two electromyography (EMG) responses—an early M wave and later H wave. The M response is elicited by direct activation of motor axons, thus bypassing spinal circuits. The H wave is an EMG response of the plantar muscle that results from synaptic activation of motor neurons by muscle afferents. H-reflex data are represented as H_{max}/M_{max}; this ratio is calculated based on threshold for both the M and H waves.

Magnetic resonance imaging. MRI studies were performed using a 7-T Biospec 70/30 USR (Bruker Corporation, Ettlingen, DE), equipped with a B-GA12 gradient coil insert and 7.2-cm inner diameter radiofrequency (RF) volume coil. Rats were oriented in prone position, ventral side down, on a custom slider bed, with isoflurane delivered at 1.8% to a nose cone. A respiratory trace was provided using a pneumatic pillow and the SA II physiologic monitoring system (Small Animal Instruments, Inc., Stony Brook, NY). Magnetic resonance scanning consisted of respiratory-gated multi-parametric scanning in a sagittal plane, which bisected the length of the cord, with shared geometric features between acquisitions (0.2×0.2 mm in-plane resolution over a 40×40 mm field of view, 1-mm slice thickness). Acquisitions consisted of a T2-weighted rapid acquisition with relaxation enhancement T2-weighted image set (echo time [TE] 80 ms; repetition time [TR] matched to respiratory rate; 18 average, 5 min 24 sec at 40 breaths per minute), T2 mapping (64 evenly spaced TEs between 12 and 768 ms; successive repetitions triggered by first breath beyond 8 sec, two averages; 40+-min scan time), and magnetization transfer ratio (MTR) mapping by sequential two-dimensional fast low-angle shot acquisitions with and without MT contrast (4.9-ms TE, 39.9-ms TR, 30-degree flip angle, 40 averages, 5 min 20 sec per image). MT contrast was generated using a 27-ms Gaussian-shaped RF pulse applied at 3 kHz off-resonance with 10-μT peak RF amplitude.

T2 and MTR map processing used custom MATLAB scripts (The MathWorks, Inc., Natick, MA). Regions of interest (ROIs) characteristic of core and peripheral regions of injury as well as remote cord were drawn manually using MIPAV software (National Institutes of Health, Bethesda, MD), considering contrast patterns in all three acquisitions by visualization of ROI copied across image sets. Mean and standard deviations of T2 and MTR were calculated using MIPAV histogram analysis functionality.

Statistical analysis

All statistical analysis was performed using SigmaStat software (SSPS, Inc., Chicago, IL). All data are represented as the mean ±

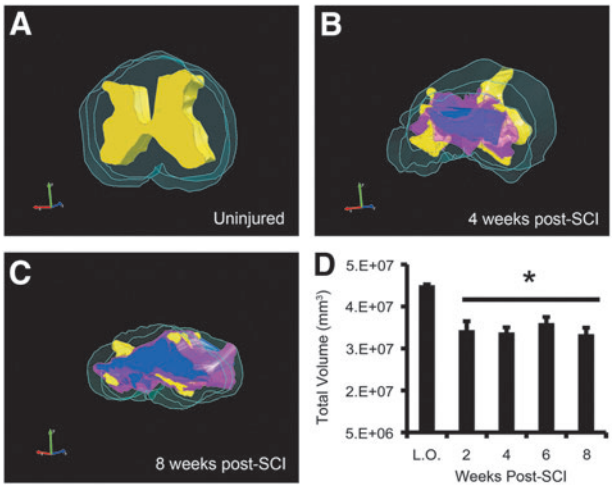

FIG. 1. Total cord volume decreases as a result of injury. (**A**) Three-dimensional (3D) reconstruction of the uninjured cord showing gray matter (yellow) and white matter (green). 3D reconstructions through the injury epicenter at 4 (**B**) and 8 weeks post-injury (**C**). Lesional tissue = pink; cavity = blue. 3D reconstructions were generated based on three histological sections that represent a 1-mm region of the cord. (**D**) Quantification of total cord volume (absolute numbers) shows a significant decrease at all time points postinjury. Asterisk indicates values that are significantly different from laminectomy-only animals (L.O.), as determined by two-way analysis of variance with Tukey's post-hoc test ($p < 0.05$). $n = 3$ in laminectomy-only group; $n = 4$ in each time point post-injury. Data are presented as mean ± standard error of the mean. SCI, spinal cord injury. Color image is available online at www.liebertpub.com/neu

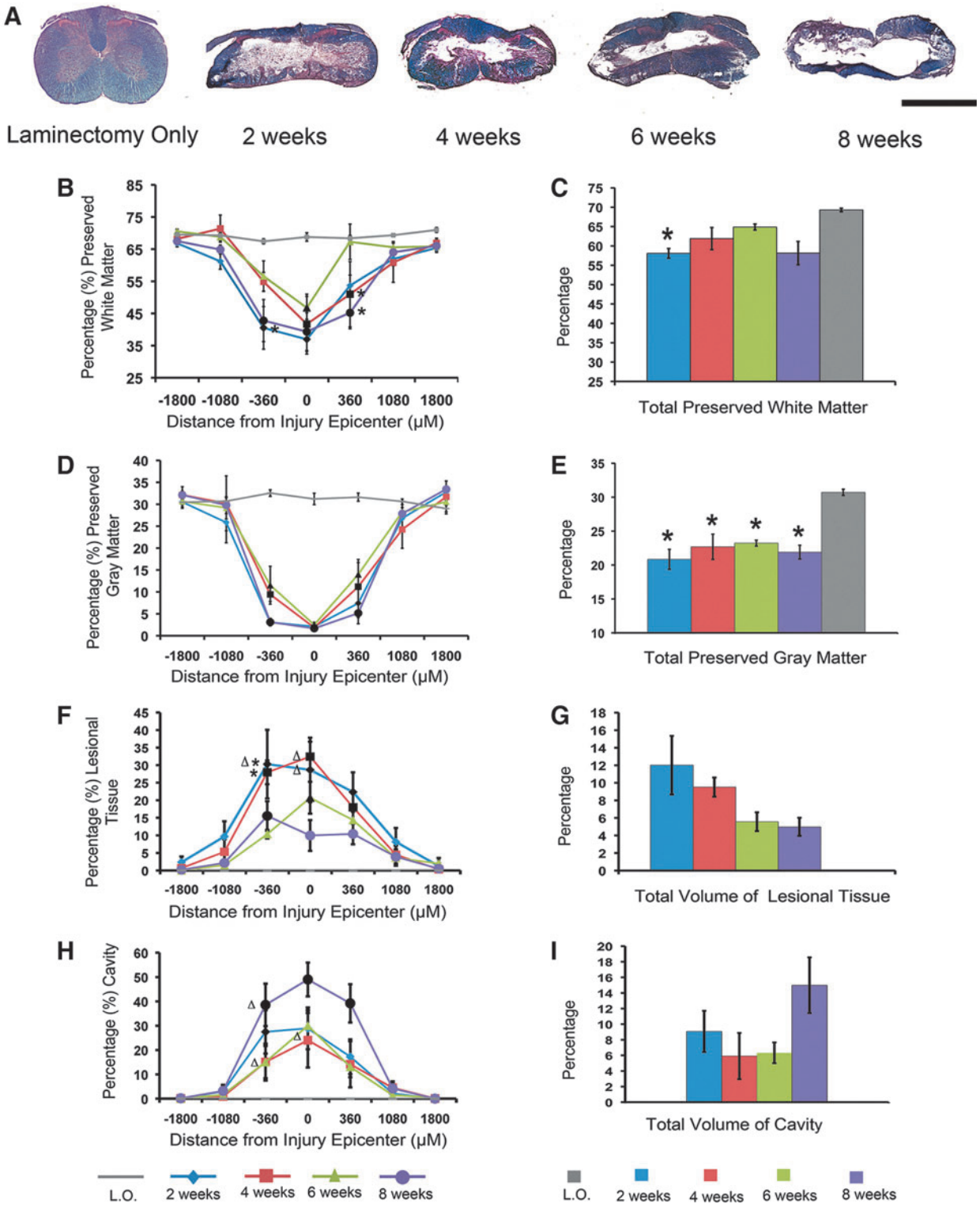

FIG. 2. Dynamic changes in the lesion after moderate clip-compression injury at C6. (**A**) Representative axial sections through the injury epicenter stained with Luxol fast blue/hematoxylin and eosin at 2, 4, 6, and 8 weeks postinjury. (**B**) White matter (WM) preservation rostral and caudal to the lesion epicenter. (**C**) Total percentage of spared WM at 2, 4, 6, and 8 weeks postinjury. (**D**) Gray matter (GM) preservation rostral and caudal to the lesion epicenter. (**E**) Injury results in a significant decrease in GM at all time points, as compared to laminectomy-only (L.O.) animals. (**F**) Percentage of lesional tissue rostral and caudal to the injury epicenter. (**G**) The volume of lesional tissue decreases as recovery proceeds. None of these decreases were statistically significant. (**H**) Percentage of cavity volume rostral and caudal to the injury epicenter. (**I**) The total volume of the cavity increases over time. None of these increases were statistically significant. (B, D, F, and H) Statistical significance was determined by a two-way analysis of variance (ANOVA) with Tukey's post-hoc analysis ($p < 0.05$). Black markers represent values that are significantly different from L.O. Single asterisks represent values that are significantly different from 6 weeks postinjury. Δ represents values that are significantly different from 8 weeks postinjury. (C, E, G, and I) Statistical significance was determined using a one-way ANOVA with Tukey's post-hoc analysis ($p < 0.05$). Single asterisks represent values that are significantly different from L.O. ($n = 3$ in L.O. group; $n = 4$ in each time point postinjury). Data are presented as mean ± standard error of the mean. Scale bar = 50 μM. Color image is available online at www.liebertpub.com/neu

standard error of the mean. After one-way analysis of variance (ANOVA) and two-way ANOVA, Tukey's post-hoc testing was applied. $p < 0.05$ was considered significant.

Results

Moderate clip-compression injury leads to gray matter loss, white matter loss, and cavity formation

In order to characterize changes in the lesion at C6 that occur over 8 weeks of natural recovery after clip-compression injury, we performed a time-course study to evaluate GM sparing, WM sparing, formation of lesional tissue, and cavity size at 2, 4, 6, and 8 weeks postinjury. We quantified these parameters by performing stereology on transverse sections stained with LFB-HE and presented the data as a percentage of total cord volume (Fig. 2). This analysis determined that whereas both total GM and WM volume decrease as a result of injury, the loss of GM is far more pronounced. Quantification of total GM demonstrated 20–30% (Fig. 2E) sparing; in contrast, up to 65% of WM is spared in total (Fig. 2C).

Previous studies from our lab have quantified the amount of lesional tissue and cavity in cervical models of injury.[16] Based on this work, lesional tissue was distinguished from surrounding unlesioned tissue by intense eosin staining and a fibrous, irregular appearance. As recovery proceeds, the volume of lesional tissue decreases (Fig. 2F,G) while the volume of the cavity increases (Fig. 2H,I). Analysis of GM and WM preservation rostral and caudal to the epicenter revealed that there is no significant difference in tissue preservation on either side of the injury (Fig. 2B,D). We observed a trend toward recovery of GM and WM at 4 and 6 weeks postinjury; this recovery effect is lost at 8 weeks postinjury, when the cavity is at its largest. Though this recovery effect is not statistically significant, it suggests that the lesion undergoes dynamic changes post-injury that could be a factor in determining a therapeutic window.

In order to determine whether the injury-induced decrease in cord volume was affecting our analysis, we examined absolute volumes of GM and WM. The volume of GM was significantly decreased at 2 ($6.18 \times 10^9 \pm 7.84 \times 10^8\ \mu M^3$), 4 ($6.6 \times 10^9 \pm 7.9 \times 108\ \mu M^3$), 6 ($7.22 \times 10^9 \pm 4.11 \times 108\ \mu M^3$), and 8 weeks ($6.27 \times 10^9 \pm 5.97 \times 10^8\ \mu M^3$), compared to laminectomy-only animals ($1.23 \times 10^{10} \pm 2.5 \times 10^8\ \mu M^3$; $p < 0.01$, one-way ANOVA followed by Tukey's post-hoc test). Similar to our initial analysis, there was no significant difference in GM volume between different time points postinjury. Statistical analysis of absolute volumes of spared WM revealed significant decreases at 2 ($1.71 \times 10^{10} \pm 1.41 \times 10^9\ \mu M^3$), 4 ($1.78 \times 10^{10} \pm 9.31 \times 10^8\ \mu M^3$), 6 ($2.01 \times 10^{10} \pm 1.08 \times 10^9\ \mu M^3$), and 8 weeks ($1.66 \times 10^{10} \pm 1.57 \times 10^9\ \mu M^3$) postinjury, as compared to laminectomy only ($2.77 \times 10^{10} \pm 1.53 \times 10^8\ \mu M^3$; $p < 0.05$, one-way ANOVA followed by Tukey's post-hoc test). Therefore, changes in total cord volume did affect our initial analysis in which WM volume was significantly decreased at 2 weeks post-injury only.

Lesion dynamics can be assessed in vivo *using quantitative T2-weighted magnetic resonance imaging*

The total volume of the cord is reduced as a result of injury, as illustrated qualitatively by 3D reconstructions in Figure 1. Quantification of total cord volume confirmed that clip-compression causes a significant decrease at all time points postinjury (Fig. 1D). Anatomical imaging of the injury epicenter using T2-weighted MRI revealed a cystic cavitation between the C6 and C7 vertebrae at all time points (Fig. 3A,D,G). The morphology of the injury epicenter observed using MRI was confirmed by taking representative histological sections (Fig. 3B,E,H) from the same animals imaged in Figure 3A,D,G. Quantitative analysis demonstrated that whereas cavity size increased over the 8-week recovery period, there was a decrease at 4 weeks post-injury (Fig. 3J). This trend was not statistically significant; however, it was consistent with increased GM and WM sparing observed at 4 weeks postinjury in our histological lesion analysis. Quantitative analysis of T2 relaxation time after C6 injury revealed that the epicenter, subpial rim of WM surrounding the epicenter, and WM distal to the injury have distinct T2 relaxation times (Fig. 3C,F,I,K). The injury epicenter is characterized by long T2 relaxation times, suggesting high water content. T2 relaxation time in the injury epicenter decreased significantly from 2 to 4 weeks post-injury. At 2 weeks postinjury, there was a statistically significant difference in T2 relaxation time between the subpial rim and WM distal to the injury site; this difference did not persist at later time points. The injury epicenter displayed the most dramatic changes in T2 relaxation time over the recovery period, as compared to the subpial rim and distal WM, which remained relatively stable over time.

Magnetization transfer magnetic resonance imaging can be used to quantify pathological changes and myelination in the injured cervical cord

This analysis demonstrated that, similar to T2 mapping, MT-MRI can be used to distinguish three different regions in the injured cord. Representative pseudocolored MTR maps showed distinct MTR values in the GM and WM of the uninjured cord (Fig. 4A) and in the epicenter, subpial rim, and WM distal to the injury at 2 (Fig. 4B), 4 (Fig. 4C), and 8 weeks (Fig. 4D). The injury epicenter had the lowest MTR (10–16%), compared to the other regions. The subpial rim of surviving WM had an MTR of 23–30%. WM distal to

FIG. 3. Lesion dynamics can be assessed using quantitative MRI. (**A**) T2-weighted mid-sagittal MRI performed at 2 weeks post-injury showing epicenter formation between C6 and C7 vertebrae. (**B**) Representative sagittal section through the injury epicenter at 2 weeks post-injury stained with LFB-HE. (**C**) Pseudocolored image showing T2 relaxation times at 2 weeks post-injury. (**D**) T2-weighted mid-sagittal MRI performed at 4 weeks postinjury. (**E**) Sagittal section stained with LFB-HE demonstrates increased lesional tissue within the epicenter at 4 weeks postinjury. (**F**) Pseudocolored image showing T2 relaxation times at 4 weeks post-injury. (**G**) T2-weighted mid-sagittal MRI showing the epicenter at 8 weeks post-injury. (**H**) Representative histological section showing lesional tissue in the injury epicenter. (**I**) Pseudocolored image illustrating T2 relaxation times at 8 weeks post-injury. (**J**) Quantification of lesion volume demonstrates an increase in cavity size over time; however, this trend is not statistically significant, as determined by one-way analysis of variance (ANOVA; $n = 3$; $p < 0.05$). (**K**) Quantification of T2-weighted maps reveals three distinct regions: injury epicenter, rim of white matter (WM) surrounding the injury epicenter, and WM distal to the injury epicenter. There was a significant decrease in T2 relaxation time in the epicenter over time ($n = 3$ for each time point; two-way ANOVA with Tukey's post-hoc test; $p < 0.005$). Single asterisks denote means that are significantly different from epicenter T2 relaxation time. Double asterisks denote mean epicenter T2 relaxation times that are significantly different from the 2-week time point. All bars represent mean ± standard error of the mean. Scale bar = 100 μm. MRI, magnetic resonance imaging; WM, white matter; SCI, spinal cord injury. Color image is available online at www.liebertpub.com/neu

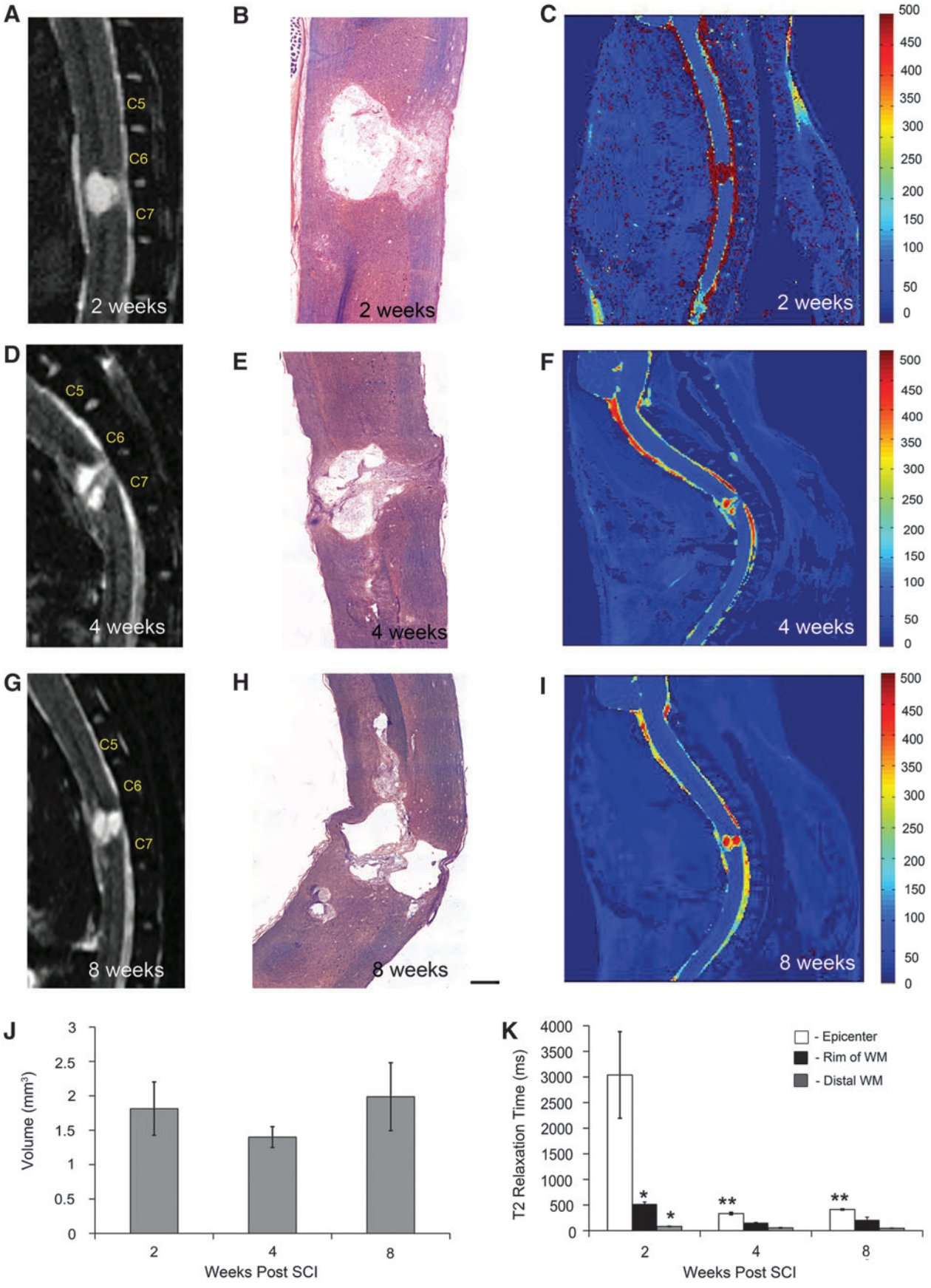
A
B
C
D
E
F
G
H
I
C5
C6
C7
2 weeks
4 weeks
8 weeks
500
450
400
350
300
250
200
150
100
50
0
J
Volume (mm³)
3
2.5
2
1.5
1
0.5
0
2
4
8
Weeks Post SCI
K
T2 Relaxation Time (ms)
4000
3500
3000
2500
2000
1500
1000
500
0
- Epicenter
- Rim of WM
- Distal WM
*
**
Weeks Post SCI

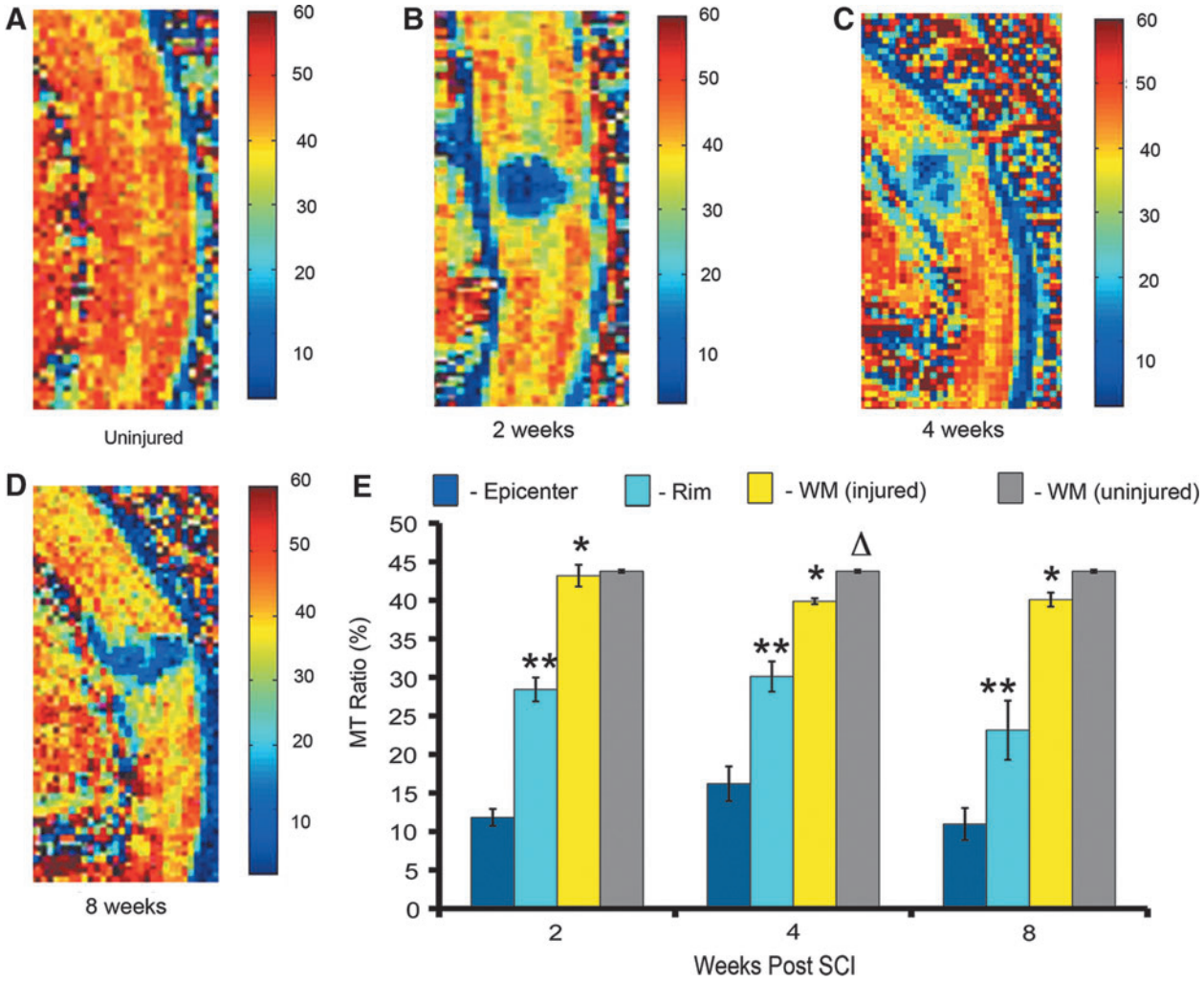

FIG. 4. Magnetization transfer magnetic resonance imaging (MT-MRI) is a noninvasive technique that can be used to quantify pathological changes in the injured cervical cord *in vivo*. (**A**) Mid-sagittal section of an uninjured cord pseudocolored to represent magnetization transfer ratios (MTRs). (**B**) Mid-sagittal section through the injury epicenter at 2 weeks post-injury. (**C**) Mid-sagittal section through the injury epicenter at 4 weeks post-injury. (**D**) Mid-sagittal section through the injury epicenter at 8 weeks post-injury. (**E**) Quantification of MTR over the recovery period shows a significant difference in MTR between three different regions in the injured cord (epicenter, rim of WM surrounding the epicenter, and WM distal to the injury), but no significant difference in the MTR of any of these regions over time (two-way analysis of variance with Tukey's post-hoc test; $n=3$ in each time point postinjury; $p<0.05$). Single asterisks indicate when MTR is significantly different from epicenter. Two asterisks indicate a significant difference between the rim of WM surrounding the epicenter and distal WM. Δ indicates that, at 4 weeks postinjury, there was a significant difference between the MTRs of WM in the injured (yellow bar) and uninjured cord (gray bar); $n=3$ in uninjured group; *t*-test; $p=0.033$). WM, white matter; SCI, spinal cord injury. Color image is available online at www.liebertpub.com/neu

the injury site had the highest MTR (39–43%; Fig. 4E). Over the recovery period, there was no significant change in the MTRs of these three regions. Studies in animal models have established that SCI results in Wallerian degeneration, demyelination, and oligodendrocyte cell death—processes that have consequences distal to the injury.[17] In order to quantitatively assess the effect of our injury on regions distant to the injury site, we compared the MTR of distal WM in the injured cord to a region of WM in the uninjured cord (Fig. 4E). In both the injured and uninjured cord, WM in the cervical region had an MTR of approximately 43%. At 4 and 8 weeks post-injury, WM MTR in the uninjured cord was slightly higher, as compared to WM in the injured cord; however, this difference was only significant at 4 weeks postinjury (*t*-test; $p=0.03$). This analysis shows that MT-MRI is a useful tool for assessing neuroanatomy in the injured cord, and that it could potentially be applied to assess myelin content in SCI models.

Moderate C6 injury results in hind- and forelimb dysfunction

We first performed open-field locomotor testing using the BBB scale. Moderate clip-compression injury at C6 reduced BBB score by more than half, compared to laminectomy animals, at 1 week post-injury (Fig. 5A). Animals displayed statistically significant improvements in BBB score over the recovery period; however, this recovery was not dramatic, with animals improving from a BBB score of 9.8 at week 1 to 11.3 at week 8. To determine whether poor behavioral improvement was a result of generalized loss of

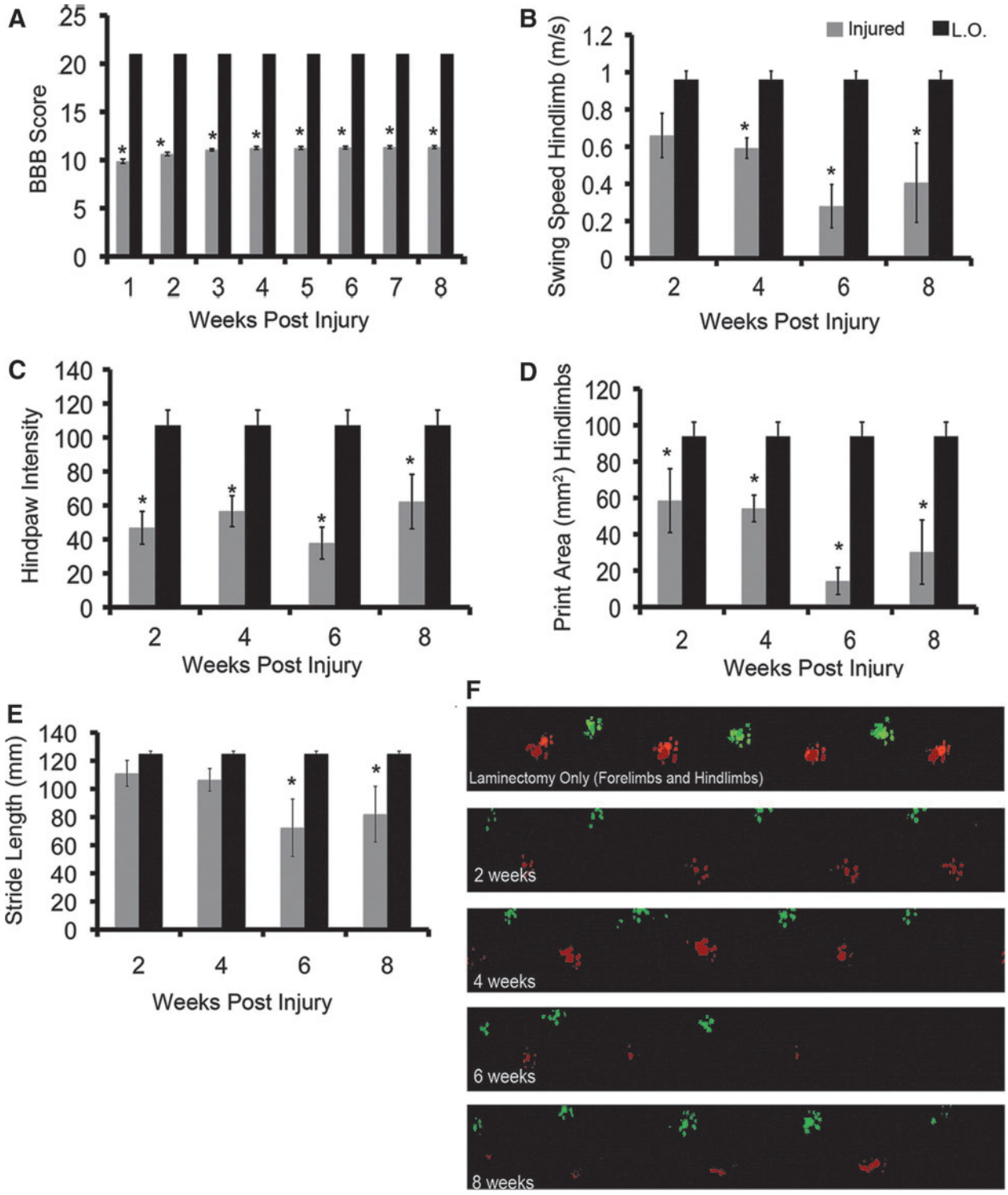

FIG. 5. Moderate C6 injury results in hindlimb dysfunction. (**A**) BBB scoring demonstrates a significant decrease in locomotor function in C6-injured animals, compared to laminectomy only controls (L.O.; two-way analysis of variance [ANOVA]; *$p < 0.001$; L.O. = 4, C6 injured = 16). In C6-injured animals at 2, 3, 4, 5, 6, 7, and 8 weeks post-injury, there was a significant improvement in BBB score, as compared to 1 and 2 weeks post-injury (Tukey's post-hoc test; $p = 0.05$). (**B**) CatWalk analysis revealed that C6 injury results in decreased swing speed in the hindlimbs. (**C**) Print intensity is reduced in the hindlimbs of C6-injured animals at all time points. (**D**) Print area is significantly reduced in C6-injured animals at all time points postinjury. At 6 weeks post-injury, print area is significantly decreased (Tukey's post-hoc test; $p = 0.043$), as compared to 2 weeks post-injury. (**E**) Hindlimb limb stride length is not significantly reduced, compared to uninjured animals, until 6 and 8 weeks post-injury. (**F**) Pseudocolored paw prints showing representative walking patterns for laminectomy animals and animals that are 2, 4, 6, and 8 weeks post-injury. For laminectomy only, both fore- and hindlimb prints are shown; for injured animals, only hindlimb prints are represented (CatWalk analysis: $n = 4$ in the laminectomy-only group and $n = 5$ in the C6-injured group; two-way ANOVA with Tukey's post-hoc test; $p < 0.05$). All data are represented as mean ± standard error of the mean. Asterisks represent values that are significantly different from laminectomy-only animals. Black bars represent laminectomy-only, and gray bars represent C6-injured animals. BBB, Basso, Beattie, and Bresnahan. Color image is available online at www.liebertpub.com/neu

neuromuscular function, we performed inclined plane testing. This parameter showed significant improvement over the recovery period (Supplementary Fig. 1) (see online supplementary material at http://www.liebertpub.com/neu).

In order to better understand deficits in hindlimb function that result from C6 injury, we performed CatWalk analysis. Previous work in our lab has established a methodology for using CatWalk to quantify locomotor deficits in SCI models.[18–20] Hindlimb swing speed was decreased by approximately 60% in C6-injured animals at 2 and 4 weeks post-injury (Fig. 5B). Swing speed was further decreased at 6 weeks post-injury to approximately 30%, compared to laminectomy-only animals; however, this decrease was not statistically significant, when compared to the 2- and 4-week time points (two-way ANOVA with Tukey's post-hoc test; $p = 0.05$). Hindpaw intensity showed a significant reduction in C6-injured animals at all time points (Fig. 5C). C6 injury results in a significant decrease in hindpaw print area at all time points. Print area decreases significantly over time. At 2 and 4 weeks postinjury, print area is decreased by 40%, as compared to laminectomy-only animals; this decrease continues at 6 weeks postinjury, where print area is reduced by 80% (Fig. 5D). Representative images of paw prints display a clear decrease in print area and intensity over the recovery period (Fig. 5F).

One of the primary aims in developing our model was to mirror the loss of upper-limb function observed in human cSCI. We therefore performed a detailed analysis of forelimb function. Grip testing showed that injury reduces upper-limb strength by over half, compared to laminectomy-only animals (Fig. 6A), and that animals do not display any significant improvement in function over the recovery period (two-way ANOVA with Tukey's post-hoc test; $p < 0.05$). Analysis of forepaw parameters obtained using CatWalk demonstrated a significant decrease in print area, width, and length in C6-injured animals (Fig. 6B,C,D). At 2 and 4 weeks postinjury, print area was decreased by approximately 40%; at 6 and 8 weeks post-injury, this effect was doubled, with print area being reduced by 80%, compared to laminectomy-only animals. The decrease in print area over the recovery period was statistically significant (two-way ANOVA with Tukey's post-hoc test; $p < 0.05$); however, this trend was not observed in our analysis of print width and length. Though print width and length were reduced at later time points, they did not display a statistically significant decline. Similar to the trend observed in the hindlimbs, forelimb swing speed was decreased significantly at all time points postinjury (Fig. 6E). Forepaw print intensity was significantly reduced at all time points in C6-injured animals (Fig. 6G). Forelimb stride length was reduced by approximately 60% in C6-injured animals; however, this parameter remained relatively stable over the recovery period (Fig. 6H).

As observed in our analysis of hindlimb parameters, representative paw prints show a decrease in print area and intensity over time (Fig. 6F). Overall, analysis of paw statistics suggests similarities in functional deficits of the fore- and hindlimbs.

Moderate C6 injury results in a significant decrease in forelimb sensory-evoked potential amplitude and an increase in sensory-evoked potential latency and hindlimb H-reflex

To investigate the effects of injury on forelimb sensory function, we analyzed forelimb SEPs at the end of the recovery period. Recordings were obtained from C1–C2 after forepaw stimulation (Fig. 7A). Peak amplitude, measured from the first positive to the first negative peak, was reduced by more than half in C6-injured animals at 8 weeks post-injury (t-test; $p = 0.019$; Fig. 7B,C). Further, peak latency was increased in C6-injured animals (t-test; $p = 0.020$; Fig. 7B,D). Increased spasticity below the level of injury is commonly associated with cSCI in humans; therefore, we measured H-reflex in the hindlimbs of C6-injured animals. H reflex provides a measure of motor neuron excitability and acts as an indicator of spasticity. We expressed the maximum H-reflex as a ratio of the H_{max}/M_{max}. At 8 weeks postinjury, hindlimb H-reflex in C6-injured animals was increased by almost 3-fold, compared to laminectomy-only animals (t-test; $p = 0.042$; Fig. 7E,F).

Discussion

The SCI community has identified the development of cervical models of injury as imperative for improving success in clinical translation of potential therapies.[21,22] Approximately 70% of all traumatic cervical injuries result in incomplete lesions.[23] Here, we present a rat model of bilateral incomplete cSCI that has neurobehavioral and -anatomical similarities to this condition in humans. In addition, we have developed MRI protocols for assessing the injured rat spinal cord that will be useful tools in analyzing the effects of therapies in our model. Previous work has established that acute trauma to the spinal cord, followed by continued compression, triggers a cascade of secondary injury events that result in GM necrosis, WM damage, and cyst formation.[24] The Rivlin-Tator aneurysm clip was originally designed for use in the thoracic cord;

FIG. 6. Moderate clip-compression injury at C6 results in forelimb dysfunction. (**A**) C6-injured animals display significantly decreased grip strength, compared to laminectomy-only (L.O.) animals (two-way analysis of variance [ANOVA]; $p < 0.001$; injured = 16, L.O. = 4). There was no significant improvement in grip strength over the recovery period (Tukey's post-hoc test; $p < 0.05$). (**B**) CatWalk analysis demonstrated a significant decrease in forepaw print area at all time points (two-way ANOVA; $p < 0.05$). There was a significant decrease in print area from 2 and 4 weeks post-injury to 6 and 8 weeks post-injury (Tukey's post-hoc test; $p < 0.05$). (**C**) The decrease in print area is supported by a significant decrease in forepaw print width (two-way ANOVA; $p < 0.001$). There is a significant decrease in print width between 4 and 8 weeks post-injury (Tukey's post-hoc test; $p = 0.026$). (**D**) In C6-injured animals, print length was significantly lower at 6 and 8 weeks postinjury (two-way ANOVA; $p < 0.05$). Print length decreased significantly from 4 weeks post-injury to 6 and 8 weeks post-injury (Tukey's post-hoc test; $p < 0.05$). (**E**) Forepaw swing speed is significantly reduced at all time points (two-way ANOVA; $p < 0.05$). There was no statistically significant decline in swing forepaw swing speed over the recovery period (Tukey's post-hoc test; $p < 0.05$). (**F**) Representative walking patterns pseudocolored to illustrate right and left paws. Top strip shows forelimb (F.L.) and hindlimb (H.L.) paw prints in a laminectomy-only animals. For 2-, 4-, 6-, and 8-week time points, only the forelimbs are shown. C6-injured animals display decreased stride length beginning at 2 weeks post-injury. Print area and intensity are progressively reduced as recovery proceeds. (**G**) Forelimb print intensity is reduced in C6-injured animals, suggesting difficulty with weight support (CatWalk analysis: $n = 4$ in laminectomy-only group and $n = 5$ in C6-injured group). (**H**) Forelimb stride length is decreased by injury at all time points (two-way ANOVA; $p < 0.05$; CatWalk analysis: $n = 4$ in laminectomy-only group and $n = 5$ in C6-injured group). Asterisks represent values that are significantly different from laminectomy only. Black bars represent laminectomy-only and gray bars represent C6-injured animals. Data are represented as mean ± standard error of the mean. Color image is available online at www.liebertpub.com/neu

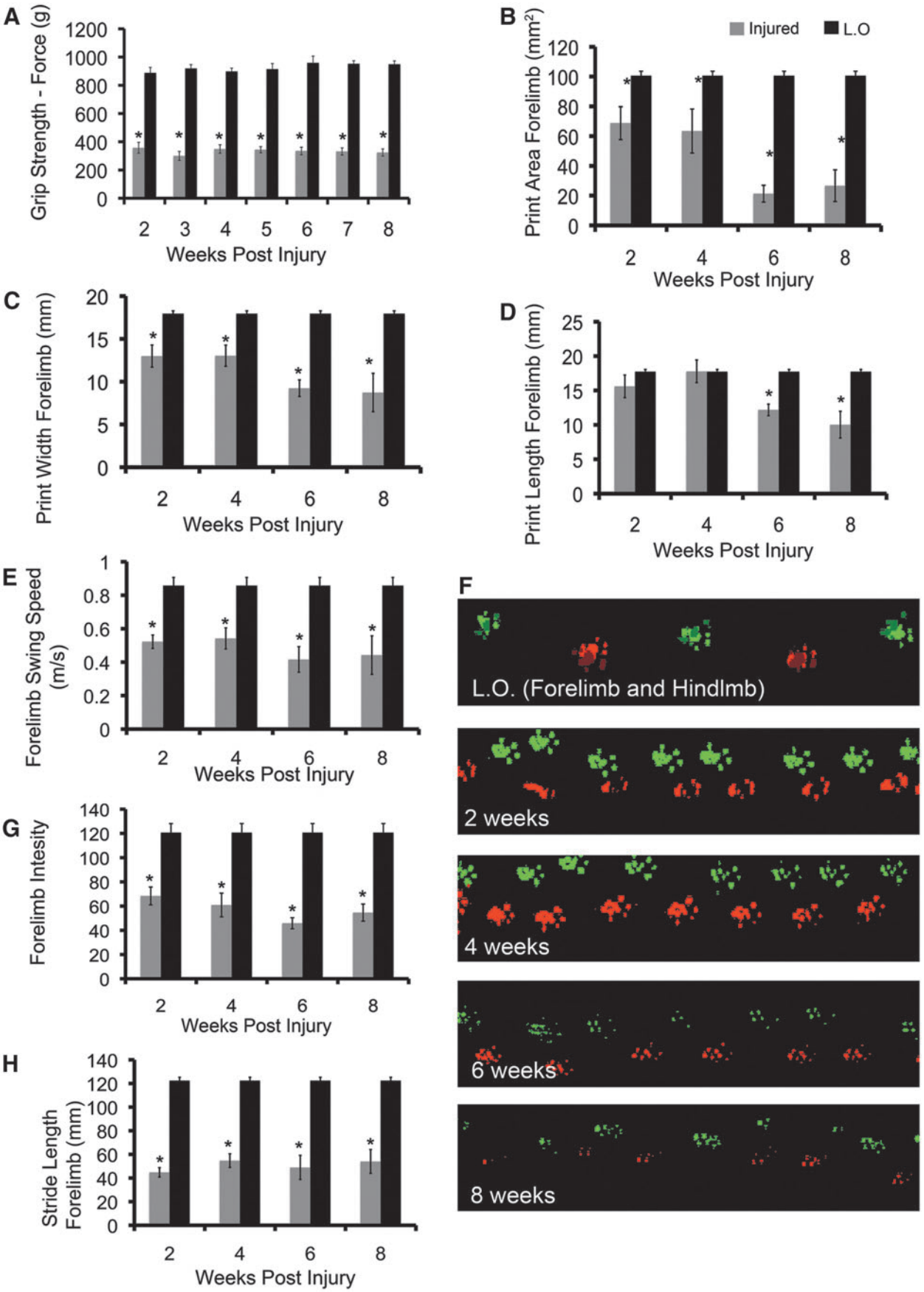
A
Grip Strength - Force (g)
1200
1000
800
600
400
200
0
2 3 4 5 6 7 8
Weeks Post Injury
B
Print Area Forelimb (mm²)
Injured
L.O
120
100
80
60
40
20
0
2 4 6 8
Weeks Post Injury
C
Print Width Forelimb (mm)
20
15
10
5
0
2 4 6 8
Weeks Post Injury
D
Print Length Forelimb (mm)
25
20
15
10
5
0
2 4 6 8
Weeks Post Injury
E
Forelimb Swing Speed (m/s)
1
0.8
0.6
0.4
0.2
0
2 4 6 8
Weeks Post Injury
F
L.O. (Forelimb and Hindlmb)
2 weeks
4 weeks
6 weeks
8 weeks
G
Forelimb Intesity
140
120
100
80
60
40
20
0
2 4 6 8
Weeks Post Injury
H
Stride Length Forelimb (mm)
140
120
100
80
60
40
20
0
2 4 6 8
Weeks Post Injury

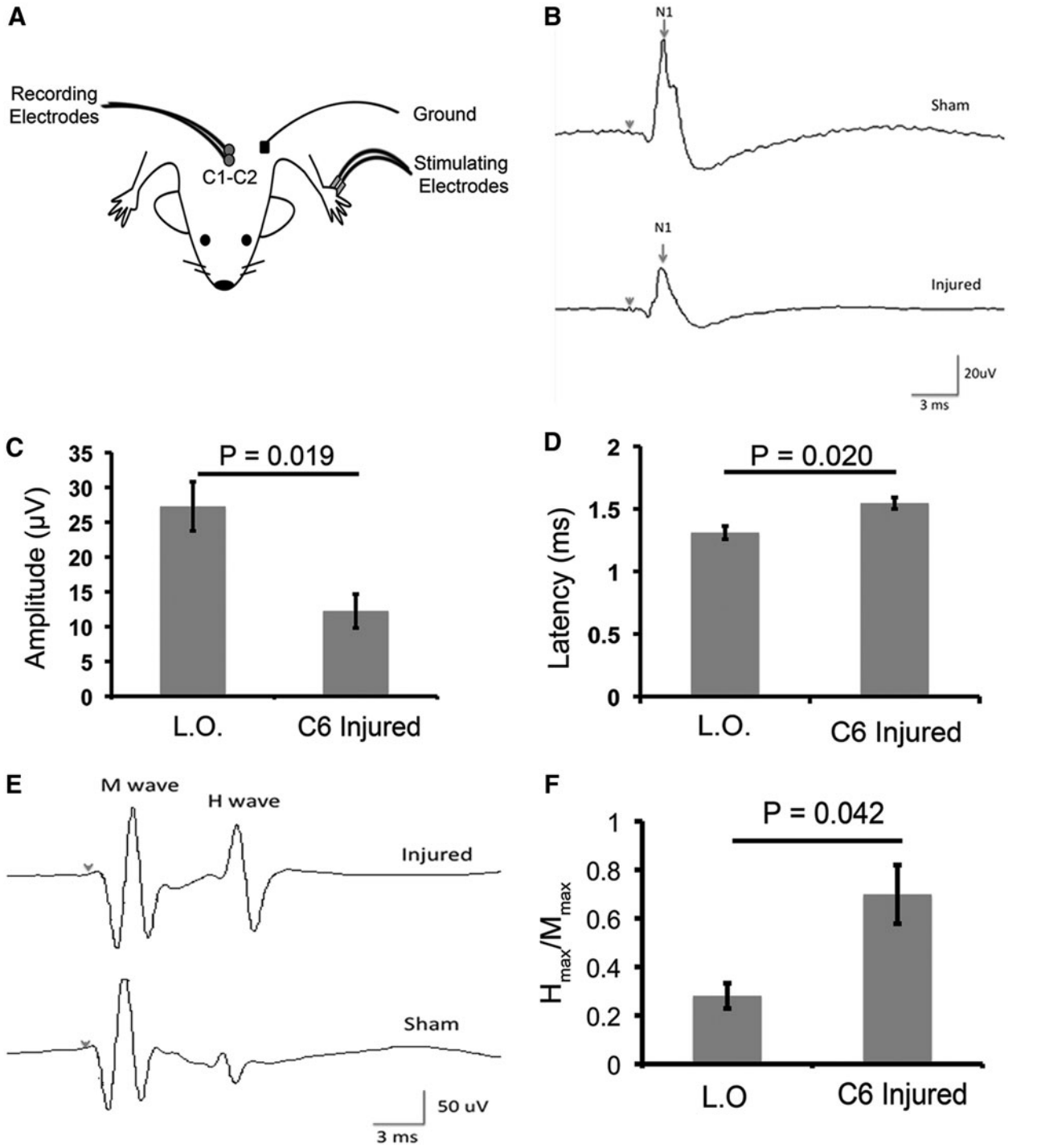

FIG. 7. Moderate C6 clip-compression injury results in a significant decrease in forelimb sensory-evoked potentials (SEPs) and an increase in hindlimb H-reflex. (**A**) Schematic depicting the strategy for recording SEPs. (**B**) Representative waveforms are shown for animals having received a laminectomy-only (L.O.; sham) and animals that are 8 weeks post-injury. (**C**) Forelimb SEPs demonstrate a significant decrease in peak amplitude in C6-injured animals 8 weeks post-injury, as compared to sham (uninjured = 4; 8 weeks post-SCI [spinal cord injury] = 6; *t*-test: $p = 0.019$). (**D**) Analysis of SEPs in the forelimbs showed a significant increase in peak latency in animals that were 8 weeks post-injury, compared to sham animals (uninjured = 4; 8 weeks post-SCI = 6; *t*-test: $p = 0.020$). (**E**) Representative waveforms of H reflex are shown for animals having received an L.O. and animals that were 8 weeks post-injury. (**F**) Excitability of hindlimb H-reflex was determined by testing the maximal plantar H-reflex and maximal plantar M response to obtain a ratio (H_{max}/M_{max}). This analysis showed a significantly lower excitability threshold in sham animals, compared to animals 8 weeks post-injury (uninjured = 4; 8 weeks post-SCI = 6; *t*-test: $p = 0.042$). Data are presented as mean ± standard error of the mean.

our lab has developed modified protocols for its use at the C6–C7 and C7–T1 spinal levels.[16,18,25] The current study represents one of the first detailed characterizations of the consequences of clip-compression injury at the C6 level in rats. Neuroanatomical analysis at multiple time points post-injury has provided important insights into the pathophysiology of secondary injury after acute impact and sustained compression in the cervical cord. The observation of increased tissue sparing at 4 and 6 weeks post-injury suggests that the late subacute and early intermediate stages of secondary injury may be associated with limited neuroanatomical recovery.

The loss of this recovery effect and increase in cavity size at 8 weeks post-injury confirms that, similar to the thoracic cord, the late intermediate phase of injury in the cervical cord is associated with tissue loss and cavity formation. These observations could have implications for determining the timing of therapeutic intervention.

In humans with incomplete cSCI, analysis of upper- and lower-extremity motor scores has revealed that the upper and lower limbs have distinct recovery profiles.[26] More specifically, upper-limb recovery is hampered by persistent weakness, whereas recovery in the lower limbs is not.[27] Closer analysis of our neurobehavioral data revealed differences in fore- and hindlimb recovery profiles. Comparison of the results from BBB scoring and grip strength testing provide the strongest evidence for a difference in hind- and forelimb recovery profiles. The lack of improvement in grip strength is an indication that forelimb recovery is not as robust as hindlimb recovery. We further explored differences in the fore- and hindlimbs by performing a detailed analysis of paw statistics obtained using CatWalk. The majority of parameters demonstrated similar decreases in fore- and hindlimb function. Stride length was one of the only parameters that had a larger decrease in the forelimbs, as compared with the hindlimbs. At 2 weeks post-injury, forelimb stride length was decreased by over 60% with no change over the recovery period (Fig. 6H). In contrast, hindlimb stride length was decreased by only 11% at 2 weeks post-injury, with a maximum decrease of 40% at 6 weeks postinjury (Fig. 5E). This difference is in accord with previous work showing that forelimb stride length is more severely affected by contusion injury.[28]

We assert that hind- and forelimb recovery are governed by different mechanisms and therefore have different recovery patterns. For instance, forepaw gripping requires sensory feedback from cutaneous mechanoreceptors.[29] Our analysis of forelimb SEPs supports the assertion that decreased forelimb sensory function contributes to the lack of recovery in grip strength. In primates and rodents there is evidence for the role of spinal interneurons in regulating hand movements.[30–32] Our injury paradigm results in significant loss of GM in the C6 region, which contains motor neurons and interneurons that make up spinal circuits responsible for forelimb and hand movement. We propose that permanent neuronal loss in forelimb spinal circuits results in functional deficits that cannot be overcome by natural recovery.

Although neurobehavioral analysis showed differences in fore- and hindlimb recovery, many paw statistics parameters suggested a similar trend toward decreased function in both fore- and hindlimbs. We hypothesize these similar trends are reflective of the development of neuropathic pain. Declining print area, width, and length in both fore- and hindpaws is indicative of a decreased ability to place pressure on the paw and thus to support weight—these two parameters are reflected by print intensity.[13] Decreased print intensity has been correlated with increased mechanical allodynia in a rat model of neuropathic pain.[33] Moreover, work from our lab has shown that print intensity can be used as an indicator of neuropathic pain in a rodent model of cervical spondylotic myelopathy.[20] Our data support the presence of neuropathic pain based on decreased print intensity in both the fore- and hindpaws. Further, these parameters decline over time, which is consistent with previous work in a rat model of clip compression that showed that neuropathic pain becomes pronounced 3–4 weeks post-SCI.[34]

Lower-limb spasticity develops in the chronic stages of SCI in humans, leading to pain, sleep disturbances, and decreased motor recovery.[35,36] H-reflex is a measure of alpha-motor neuron excitability as elicited by monosynaptic afferent inputs, and has been used to assess spasticity in humans and animals.[37] H-reflex recordings carried out at 8 weeks post-injury demonstrate that our model is characterized by the development of hindlimb spasticity. It is likely that increased spasticity contributes to hindlimb locomotor deficits observed in neurobehavioral analyses.

MRI provides a noninvasive *in vivo* method for observing pathology in the injured spinal cord over time and can thus be used to evaluate recovery after a therapeutic intervention. Further, MRI has the potential to be used to predict behavioral outcomes. In order to establish that MRI is a reliable biomarker in our model of cSCI, we first tested the ability of T2 relaxation time to distinguish the injury epicenter, subpial rim, and distal WM in the injured cord. This analysis revealed that, over 8 weeks of recovery, the most dynamic changes are observed in the injury epicenter, where T2 relaxation times decrease markedly from 2 to 4 weeks postinjury. Next, we sought to develop an MRI-based technique to quantify changes in myelination after injury. MT-MRI generates contrast between different tissue types using physical, as opposed to chemical, means. To achieve this effect, off-resonance RF irradiation, which preferentially saturates bound protons associated with macromolecules, is applied.[38] The result is energy transfer between bound and unbound protons, thus reducing the signal intensity of the unbound protons. The relative difference in signal intensities is expressed as the MTR. MTR has been correlated with the myelin content of tissue and used to detect demyelination as a result of disease or injury.[39,40]

In animal models, contusive thoracic SCI triggers demyelination that changes in magnitude over the course of recovery. Demyelination is a progressive and protracted process that is characterized by an early peak of axon demyelination at 24 h postinjury, a recovery period that can last over 1 year in rodents, and finally a sharp increase in the number of demyelinated axons at 15 months post-injury.[41] Based on this work, the recovery period from 2 to 8 weeks chosen for our analysis represents a period when levels of demyelination are relatively stable; this is confirmed by our observation that MTRs did not change significantly over the 8-week recovery period. These data also support the use of MT-MRI as a diagnostic tool to study potential therapies that promote remyelination in rat models of cSCI; however, future work is required to determine whether MT-MRI can detect subtle changes in myelination.

In conclusion, we have developed a clinically relevant animal model of incomplete cSCI that will prove a useful tool in the study of the molecular mechanisms that contribute to the unique consequences of injury in the cervical spinal cord, as well as in the identification of clinically relevant therapies.

Acknowledgments

The authors acknowledge Warren Foltz at the STTARR facility for his contribution to the MRI data and also Behzad Azad for his work on the animal care required for these experiments.

Author Disclosure Statement

No competing financial interests exist.

References

1. Sekhon, L.H., and Fehlings, M.G. (2001). Epidemiology, demographics, and pathophysiology of acute spinal cord injury. Spine (Phila. Pa. 1976) 26, S2–S12.
2. Marino, R.J., Ditunno, J.F., Jr., Donovan, W.H., and Maynard, F., Jr. (1999). Neurologic recovery after traumatic spinal cord injury: data from the Model Spinal Cord Injury Systems. Arch. Phys. Med. Rehabil. 80, 1391–1396.
3. Anderson, K.D., Gunawan, A., and Steward, O. (2005). Quantitative assessment of forelimb motor function after cervical spinal cord injury in rats: relationship to the corticospinal tract. Exp. Neurol. 194, 161–174.
4. Bosch, A., Stauffer, E.S., and Nickel, V.L. (1971). Incomplete traumatic quadriplegia. A ten-year review. JAMA 216, 473–478.
5. Gensel, J.C., Tovar, C.A., Hamers, F.P., Deibert, R.J., Beattie, M.S., and Bresnahan, J.C. (2006). Behavioral and histological characterization of unilateral cervical spinal cord contusion injury in rats. J. Neurotrauma 23, 36–54.
6. Dunham, K.A., Siriphorn, A., Chompoopong, S., and Floyd, C.L. (2010). Characterization of a graded cervical hemicontusion spinal cord injury model in adult male rats. J. Neurotrauma 27, 2091–2106.
7. Kwon, B.K., Okon, E., Hillyer, J., Mann, C., Baptiste, D., Weaver, L.C., Fehlings, M.G., and Tetzlaff, W. (2011). A systematic review of non-invasive pharmacologic neuroprotective treatments for acute spinal cord injury. J. Neurotrauma 28, 1545–1588.
8. American Spinal Injury Assocation. (2011). *International Standards for the Neurological Classification of Spinal Cord Injury*, Revised 2011. American Spinal Injury Assocation: Chicago, IL.
9. Lidal, I.B., Huynh, T.K., and Biering-Sorensen, F. (2007). Return to work following spinal cord injury: a review. Disabil. Rehabil. 29, 1341–1375.
10. Anderson, K.D. (2004). Targeting recovery: priorities of the spinal cord-injured population. J. Neurotrauma 21, 1371–1383.
11. Ditunno, J.F., Jr., Cohen, M.E., Hauck, W.W., Jackson, A.B., and Sipski, M.L. (2000). Recovery of upper-extremity strength in complete and incomplete tetraplegia: a multicenter study. Arch. Phys. Med. Rehabil. 81, 389–393.
12. Basso, D.M., Beattie, M.S., and Bresnahan, J.C. (1995). A sensitive and reliable locomotor rating scale for open field testing in rats. J. Neurotrauma 12, 1–21.
13. Hamers, F.P., Koopmans, G.C., and Joosten, E.A. (2006). CatWalk-assisted gait analysis in the assessment of spinal cord injury. J. Neurotrauma 23, 537–548.
14. Meyer, O.A., Tilson, H.A., Byrd, W.C., and Riley, M.T. (1979). A method for the routine assessment of fore- and hindlimb grip strength of rats and mice. Neurobehav. Toxicol. 1, 233–236.
15. Pearse, D.D., Lo, T.P., Jr., Cho, K.S., Lynch, M.P., Garg, M.S., Marcillo, A.E., Sanchez, A.R., Cruz, Y., and Dietrich, W.D. (2005). Histopathological and behavioral characterization of a novel cervical spinal cord displacement contusion injury in the rat. J. Neurotrauma 22, 680–702.
16. Nguyen, D.H., Cho, N., Satkunendrarajah, K., Austin, J.W., Wang, J., and Fehlings, M.G. (2012). Immunoglobulin G (IgG) attenuates neuroinflammation and improves neurobehavioral recovery after cervical spinal cord injury. J. Neuroinflammation 9, 224.
17. Abe, Y., Yamamoto, T., Sugiyama, Y., Watanabe, T., Saito, N., Kayama, H., and Kumagai, T. (1999). Apoptotic cells associated with Wallerian degeneration after experimental spinal cord injury: a possible mechanism of oligodendroglial death. J. Neurotrauma 16, 945–952.
18. Iwasaki, M., Wilcox, J.T., Nishimura, Y., Zweckberger, K., Suzuki, H., Wang, J., Liu, Y., Karadimas, S.K., and Fehlings, M.G. (2014). Synergistic effects of self-assembling peptide and neural stem/progenitor cells to promote tissue repair and forelimb functional recovery in cervical spinal cord injury. Biomaterials 35, 2617–2629.
19. Karadimas, S.K., Moon, E.S., Yu, W.R., Satkunendrarajah, K., Kallitsis, J.K., Gatzounis, G., and Fehlings, M.G. (2013). A novel experimental model of cervical spondylotic myelopathy (CSM) to facilitate translational research. Neurobiol. Dis. 54, 43–58.
20. Moon, E.S., Karadimas, S.K., Yu, W.R., Austin, J.W., and Fehlings, M.G. (2014). Riluzole attenuates neuropathic pain and enhances functional recovery in a rodent model of cervical spondylotic myelopathy. Neurobiol. Dis. 62, 394–406.
21. Kwon, B.K., Hillyer, J., and Tetzlaff, W. (2010). Translational research in spinal cord injury: a survey of opinion from the SCI community. J. Neurotrauma 27, 21–33.
22. Filli, L., and Schwab, M.E. (2012). The rocky road to translation in spinal cord repair. Ann. Neurol. 72, 491–501.
23. National Spinal Cord Injury Center. (2012). Spinal cord injury facts and figures at a glance. J. Spinal Cord Med. 35, 197–198.
24. Tator, C.H., and Fehlings, M.G. (1991). Review of the secondary injury theory of acute spinal cord trauma with emphasis on vascular mechanisms. J. Neurosurg. 75, 15–26.
25. Robins-Steele, S., Nguyen, D.H., and Fehlings, M.G. (2012). The delayed post-injury administration of soluble fas receptor attenuates post-traumatic neural degeneration and enhances functional recovery after traumatic cervical spinal cord injury. J. Neurotrauma 29, 1586–1599.
26. Marino, R.J., and Graves, D.E. (2004). Metric properties of the ASIA motor score: subscales improve correlation with functional activities. Arch. Phys. Med. Rehabil. 85, 1804–1810.
27. Marino, R.J., Burns, S., Graves, D.E., Leiby, B.E., Kirshblum, S., and Lammertse, D.P. (2011). Upper- and lower-extremity motor recovery after traumatic cervical spinal cord injury: an update from the national spinal cord injury database. Arch. Phys. Med. Rehabil. 92, 369–375.
28. Hamers, F.P., Lankhorst, A.J., van Laar, T.J., Veldhuis, W.B., and Gispen, W.H. (2001). Automated quantitative gait analysis during overground locomotion in the rat: its application to spinal cord contusion and transection injuries. J. Neurotrauma 18, 187–201.
29. Witney, A.G., Wing, A., Thonnard, J.L., and Smith, A.M. (2004). The cutaneous contribution to adaptive precision grip. Trends Neurosci. 27, 637–643.
30. Bui, T.V., Akay, T., Loubani, O., Hnasko, T.S., Jessell, T.M., and Brownstone, R.M. (2013). Circuits for grasping: spinal dI3 interneurons mediate cutaneous control of motor behavior. Neuron 78, 191–204.
31. Fetz, E.E., Perlmutter, S.I., Prut, Y., Seki, K., and Votaw, S. (2002). Roles of primate spinal interneurons in preparation and execution of voluntary hand movement. Brain Res. Brain Res. Rev. 40, 53–65.
32. Takei, T., and Seki, K. (2010). Spinal interneurons facilitate coactivation of hand muscles during a precision grip task in monkeys. J. Neurosci. 30, 17041–17050.
33. Vrinten, D.H., and Hamers, F.F. (2003). 'CatWalk' automated quantitative gait analysis as a novel method to assess mechanical allodynia in the rat: a comparison with von Frey testing. Pain 102, 203–209.
34. Bruce, J.C., Oatway, M.A., and Weaver, L.C. (2002). Chronic pain after clip-compression injury of the rat spinal cord. Exp. Neurol. 178, 33–48.
35. Little, J.W., Ditunno, J.F., Jr., Stiens, S.A., and Harris, R.M. (1999). Incomplete spinal cord injury: neuronal mechanisms of motor recovery and hyperreflexia. Arch. Phys. Med. Rehabil. 80, 587–599.
36. Little, J.W., Micklesen, P., Umlauf, R., and Britell, C. (1989). Lower extremity manifestations of spasticity in chronic spinal cord injury. Am. J. Phys. Med. Rehabil. 68, 32–36.
37. Lee, H.J., Jakovcevski, I., Radonjic, N., Hoelters, L., Schachner, M., and Irintchev, A. (2009). Better functional outcome of compression spinal cord injury in mice is associated with enhanced H-reflex responses. Exp. Neurol. 216, 365–374.
38. Wolff, S.D., and Balaban, R.S. (1989). Magnetization transfer contrast (MTC) and tissue water proton relaxation in vivo. Magn. Reson. Med. 10, 135–144.
39. Wilhelm, M.J., Ong, H.H., Wehrli, S.L., Li, C., Tsai, P.H., Hackney, D.B., and Wehrli, F.W. (2012). Direct magnetic resonance detection of myelin and prospects for quantitative imaging of myelin density. Proc. Natl. Acad. Sci. U. S. A. 109, 9605–9610.
40. Gareau, P.J., Weaver, L.C., and Dekaban, G.A. (2001). In vivo magnetization transfer measurements of experimental spinal cord injury in the rat. Magn. Reson. Med. 45, 159–163.
41. Totoiu, M.O., and Keirstead, H.S. (2005). Spinal cord injury is accompanied by chronic progressive demyelination. J. Comp. Neurol. 486, 373–383.

Address correspondence to:
Michael G. Fehlings, MD, PhD
Toronto Western Hospital
University Health Network
Krembil Discovery Tower
60 Leonard Street
7KD430
Toronto, Ontario, Canada M5T 2S8

E-mail: michael.fehlings@uhn.ca